COMPARATIVE ANALYSIS AND OPTIMIZATION OF WIND TURBINE PERFORMANCE: A CASE STUDY IN NAAMA ALGERIA

Acta Energiae Solaris Sinica

Sekkal Mohammed Chakib[1,2,3], Ziani Zakarya[2,3,4] , Meliani Sidi Mohammed[1,5]

[1] University Abou Bekr Belkaid Tlemcen
[2] University Center Salhi Ahmed of Naama, Department of Electrotechnics.
[3] Laboratory for Sustainable Management of Natural Resources (GDRN).
[4] Unity for Research on Materials and Renewable Energies.
[5] Laboratory of Production Engineering, MELT.

E-mail: sekkal@cuniv-naama.dz
Received 5 April 2022, Revised 27 March2023
Published 28 May 2023
Online at https://actaenergiaesolaris.com/index.php/papers/volume-44/issue-1/189-2/

Abstract

In our work, we conducted a comprehensive analysis comparing the experimental results with the modeled performance of a wind turbine located in the Naama site in Algeria. Our primary objective was to evaluate the effectiveness and accuracy of the model in predicting the behavior of the wind turbine under real-world conditions. To begin, we calculated the wind speed variations throughout the year at the Naama site. This involved collecting meteorological data and employing mathematical calculations to determine the average and fluctuation patterns of wind speeds. Simultaneously, we carried out practical measurements of the power output using an actual wind turbine installed at the Naama Center University, specifically the Salhi Ahmed facility. Next, we employed a sophisticated program to model and simulate various physical parameters associated with the wind turbine. This encompassed factors such as blade length, turbine height, rotor diameter, and generator efficiency, among others. By inputting the meteorological data and the turbine's specifications into the program, we obtained a simulated performance profile of the wind turbine under different wind conditions. To validate the accuracy of the model, a second set of experiments was conducted in the laboratory. These experiments involved subjecting the wind turbine to controlled wind speeds and comparing the obtained results with the model's predictions. The outcomes of this test indicated a close alignment between the experimental and modeled data, reinforcing the reliability of the model. Additionally, we explored the optimization of the wind turbine design by investigating the ideal radius and the number of blades. Through extensive analysis and simulations, we evaluated various combinations of blade lengths and numbers to determine their impact on the turbine's performance. This endeavor aimed to enhance the overall efficiency and electricity production capacity of the wind turbine. The results obtained from the Naama site exhibited a significant level of satisfaction regarding the electricity production capabilities of wind farms. The comparison between the experimental and modeled data showcased a high degree of correlation, affirming the validity of the model and its potential applicability in other wind energy projects. Overall, our work involved a thorough examination of the wind turbine's performance through a combination of experimental measurements, mathematical modeling, and simulation techniques. The findings contribute to the ongoing efforts to harness renewable energy sources, particularly wind power, for sustainable electricity generation.

Keywords: Wind turbine, Modeling, Experimental analysis, Renewable energy.

1 Introduction

The measurement of power output and estimation of annual energy production are essential in assessing the performance and feasibility of mini horizontal axis wind turbines. This research aims to provide a comprehensive understanding of the power generation capabilities and potential energy production of such turbines. By conducting experimental measurements and applying statistical analysis, the annual energy production can be estimated based on the power output characteristics of the turbine. This study focuses on power output measurement, estimation of annual energy production, power curve analysis, and the concepts of effective power, usable power, and energy of a wind turbine.

Power output measurement is influenced by factors such as wind speed, turbine efficiency, and turbine characteristics. The power output is determined by converting the mechanical power into electrical power using an electrical generator connected to the turbine. The torque exerted by the turbine can be measured using a torque sensor, while the angular speed can be determined using an anemometer or by monitoring the rotation of the turbine shaft.

Estimation of annual energy production involves analyzing the statistical profile of wind speeds in the target region and the turbine's power curve. By integrating the power output over time, the energy produced by the turbine can be estimated. The power curve represents the relationship between wind speed and power output and helps determine the optimal operating range of the turbine.

Statistical analysis and probability density function play a crucial role in estimating the annual energy production. By analyzing the wind speed data and integrating the probability density function with the power curve equation, the energy production at different wind speeds can be calculated. These calculations contribute to the estimation of annual energy production.

The concepts of effective power, usable power, and energy of a wind turbine are essential for assessing its performance and estimating annual energy production. Effective power represents the actual power captured by the turbine, while usable power refers to the portion of effective power that can be converted into electrical energy. The estimation of energy produced by the turbine involves integrating the usable power over a given period.

The capacity factor is another important measure that indicates the actual energy production of a wind turbine compared to its maximum potential. It considers factors such as start-up speed, rated speed, and cut-out speed.

In the experimental work, the objective is to determine the relationship between electrical power and wind speed under controlled laboratory conditions. The materials and methods section describes the test bench used, including the combined RE580 test bench consisting of a mini horizontal axis wind turbine and a photovoltaic panel. The installation, commissioning, and operation procedures are outlined to ensure accurate data collection.

2 Measurement of Power Output and Estimation of Annual Energy Production of Mini Horizontal Axis Wind Turbine

The measurement of power output and estimation of annual energy production are crucial in evaluating the performance and feasibility of mini horizontal axis wind turbines. This research aims to provide a comprehensive understanding of the power generation capabilities and potential energy production of such turbines. The study involves experimental measurements

and statistical analysis to estimate the annual energy production based on the power output characteristics of the turbine[5].

2.1 Power Output Measurement:

The power output of a mini horizontal axis wind turbine is influenced by several factors, including wind speed, turbine efficiency, and turbine characteristics. To measure the power output, an electrical generator connected to the turbine converts the mechanical power into electrical power. The generated electrical power can be determined using the formula[6]:

$$\text{Power (P)} = \text{Torque (T)} \times \text{Angular Speed } (\omega) \qquad \text{Equation 1}$$

Where:
P: Power output in watts (W)
T: Torque exerted by the turbine in newton-meters (Nm)
ω: Angular speed of the turbine in radians per second (rad/s)

The torque exerted by the turbine can be measured using a torque sensor, and the angular speed can be determined using an anemometer or by monitoring the rotation of the turbine shaft[7].

2.2 Estimation of Annual Energy Production:

The estimation of annual energy production involves considering the power output of the turbine over an extended period. By analyzing the statistical profile of wind speeds in the target region and the turbine's power curve, an estimate of the annual energy production can be derived.

The energy produced by the turbine can be calculated by integrating the power output over time. Assuming a constant time interval (Δt) and considering the discrete power measurements at different time intervals (Pi), the energy produced (E) can be estimated as follows[8]:

$$E = \Sigma(Pi \times \Delta t) \qquad \text{Equation 2}$$

Where:
E: Energy produced by the turbine in watt-hours (Wh)
Pi: Power output at time interval i in watts (W)
Δt: Time interval between measurements in hours (h)

To estimate the annual energy production, Equation 2 is applied over the course of one year, considering the wind speed distribution and power output variations during that period.

2.3 Power Curve Analysis:

The power curve of a mini horizontal axis wind turbine represents the relationship between wind speed and power output. It provides insights into the turbine's performance across different wind speeds. The power curve can be constructed by collecting power output data at various wind speeds and fitting a mathematical function to the data.
The power curve equation typically takes the form:

$$\text{Power (P)} = C1 \times \text{Wind Speed (V)}\text{^}C2 \qquad \text{Equation 3}$$

Where:
P: Power output in watts (W)
V: Wind speed in meters per second (m/s)
C1 and C2: Constants determined through curve fitting analysis

The power curve analysis helps in determining the range of wind speeds in which the turbine operates optimally and produces the maximum power output[9].

Statistical Analysis and Probability Density Function:
Statistical analysis plays a crucial role in estimating the annual energy production of a mini horizontal axis wind turbine. It involves analyzing the wind speed data collected from the target region to determine the probability density function (PDF) of wind speeds.
The PDF represents the distribution of wind speeds and their corresponding probabilities. By integrating the PDF with the power curve equation, the energy production at different wind speeds can be calculated. This information can then be used to estimate the annual energy production[8][10].

2.4 Effective Power, Usable Power, and Energy of a Wind Turbine

In this study, we focus on measuring the effective power, usable power, and estimating the energy produced by a wind turbine. These parameters are essential for assessing the performance of a wind turbine and estimating its annual energy production. We examine the concepts of effective power, usable power, and utilize specific equations to calculate the energy produced[11].

2.4.1 Effective Power of the Wind Turbine:

The effective power of a wind turbine represents the actual power captured by the turbine at a given moment. It depends on several factors, including wind speed and turbine characteristics. The effective power (Peff) can be calculated using the following equation[12]:

$$Peff = 0.5 * \rho * A * V^3 * Cp \qquad \text{Equation 4}$$

Where:
Peff: Effective power in watts (W)
ρ: Air density in kilograms per cubic meter (kg/m^3)
A: Swept area of the turbine blades in square meters (m^2)
V: Wind speed in meters per second (m/s)
Cp: Power coefficient of the wind turbine (dimensionless)

The power coefficient (Cp) depends on the design and performance of the wind turbine.

Usable Power of the Wind Turbine:
Usable power represents the portion of the effective power that can actually be converted into electrical energy. It is influenced by the limitations of the turbine, such as the startup speed and maximum speed. The usable power (Putil) can be calculated using the following equation[13]:

$$Putil = Peff * \eta g * \eta m \qquad \text{Equation 5}$$

Where:
Putil: Usable power in watts (W)
ηg: Generator efficiency (dimensionless)
ηm: Gearbox efficiency (dimensionless)

The generator efficiency (ηg) and gearbox efficiency (ηm) are specific parameters of the wind turbine used.

Estimation of Energy Produced by the Wind Turbine:
The energy produced by the wind turbine can be calculated by integrating the usable power over a given period of time. The energy produced (E) can be estimated using the following equation[14]:

$$E = \int(Putil * dt) \qquad \text{Equation 6}$$

Where:
E: Energy produced by the wind turbine in joules (J) or kilowatt-hours (kWh)
Putil: Usable power in watts (W)
dt: Time interval in seconds (s) or hours (h)

Estimating the energy produced over a year requires integrating Equation 6 over a time period corresponding to one year.

2.4.2 Capacity Factor:

The capacity factor (CF) is a measure of the actual energy production of a wind turbine compared to its maximum potential. It takes into account the wind turbine's start-up speed, rated speed, and cut-out speed. The capacity factor can be calculated using the following equation[15]:

$$CF = (E / (365 * 24 * Peff\_max)) * 100 \qquad \text{Equation 4}$$

Where:
CF: Capacity factor as a percentage
E: Energy produced by the wind turbine in kilowatt-hours (kWh) over a year
Peff_max: Maximum effective power of the wind turbine in kilowatts (kW)

Power Measurements:

Time (hours)	Wind Speed (m/s)	Effective Power (W)	Usable Power (W)
1	3.5	2500	2100
2	4.2	3500	2800
3	2.8	1800	1500
4	5.1	4500	3600
5	3.9	3000	2400

Tab. 1 Exemple of wind turbine performance[15].

Note: The values in the table are for illustrative purposes only and may not reflect actual wind turbine performance.

This table provides a snapshot of power measurements taken at different time intervals, corresponding wind speeds, and the calculated effective power and usable power based on the given equations.

By analyzing the data from power measurements and applying the equations described above, one can assess the performance of the wind turbine, estimate its annual energy production, and evaluate its efficiency in converting wind power into usable electrical energy[16].

3 Experimental work:

The aim is to experimentally determine the relationship between electrical power and wind speed under laboratory conditions (no climate variations, no sand particles in the wind, etc.).
The objective is to obtain the most accurate estimation of the annual electrical power produced by combining this characteristic with the statistical profile of wind speeds in the studied region.
The perspective is to have data both upstream and downstream of the system in order to be able to model it.

3.1 Materials and methods:

The mini-wind turbine used is derived from the combined RE580 test bench, consisting of a horizontal-axis wind turbine and a photovoltaic panel from the English company P.A. Hilton Ltd (Hilton 2022).
The mechanical and electrical characteristics of the turbine, as well as the necessary experimental procedures for understanding this stage, are summarized below. All this information is taken from the manual provided by the manufacturer[17].

3.1.1 Combined RE580 test bench – Overview

The combined test bench for a wind turbine and a photovoltaic panel allows for the study of the fundamental principles of wind and solar energy production from wind and sunlight in a laboratory environment.
A small charge controller mounted on the bench provides instrumentation to both systems and also contains a dedicated battery charge controller that automatically regulates the wind turbine when the battery is fully charged. The console communicates between the wind turbine/photovoltaic panel and the battery provided with the bench. Both generators and the battery operate at a nominal voltage of 13.8 V (DC), and loads suitable for DC can be directly connected to the generators, with their consumption measured using an ammeter/multimeter.
The wind turbine has two speed measurement locations indicated on its housing. One is located in a free-flow area to measure the local air velocity (wind speed), and the second is located behind the wind turbine to determine the reduction in air velocity. A tachometer is provided with the wind turbine to measure the rotation speed of the turbine. A small reflector is provided to be attached to the back of the turbine hub to reflect the signal and allow the tachometer to calculate the rotation speed[18].
The combined wind turbine and photovoltaic panel test bench is designed to operate both indoors and outdoors, with a mobile charge controller, instrumentation, and power cable. The charge controller and battery are designed for laboratory use but can also be used outside depending on local weather conditions. The system instrumentation and battery are not designed to operate in a humid or rainy environment.

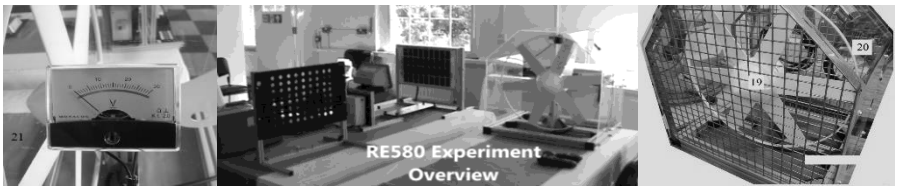

Fig. 1 Overview of the Combined Wind Turbine - Photovoltaic Panel Test Bench
The Mini Wind Turbine with its Transparent Protective Housing and Built-in Voltmeter

3.1.2 The Horizontal Axis Mini Wind Turbine: Nomenclature and Description

The figures above show the mini wind turbine of the test bench and the necessary equipment used during experimentation. Unused equipment is not detailed.

The bench's horizontal axis mini wind turbine has a diameter of 500 mm and is equipped with multiple blades (06 blades). It has a three-phase alternating current generator (19) and a rectifier to convert the three-phase current into direct current integrated into the generator head. The turbine is protected by a Plexiglas housing surrounding its top and sides and can be rotated from any angle relative to the wind to study the effect of orientation on the turbine's performance[19].

The housing has two measurement points at the front and rear for conducting air velocity measurements. These are labeled accordingly in the photographs. The air velocity measurement point at the front is designed to measure the local wind speed before the turbine. The air velocity measurement point (after the turbine) is designed to measure the air speed behind the wind turbine after kinetic energy has been extracted by the blades[20].

A strip reflector is attached to the back of the turbine at the hub level, allowing the operator to measure the rotation speed of the turbine without disturbing the airflow, which would occur if the measurement were taken at the front of the blades. An optical tachometer is available for this purpose.

The power provided by the generator is displayed on the display located at the front of the charge controller and can be accessed by scrolling through the menu using the controller's selection button.

The voltage is also indicated on the voltmeter mounted on the protective housing and is specifically used for unregulated high-speed testing[19].

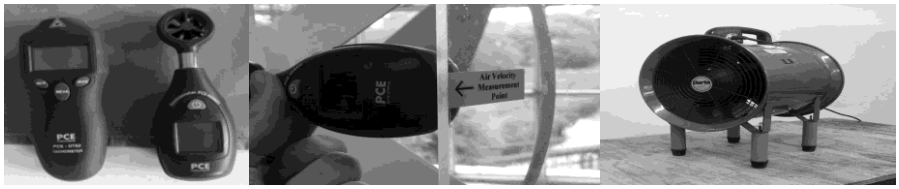

Fig. 2 The laser tachometer and anemometer are used at the airspeed measurement point (front) with a wind generator (ventilator)

The figures above show the charge controller contains the generator controller for the panel/wind turbine/battery, as well as additional instrumentation to enable testing of each individual subsystem or control of the entire structure.
On the front panel of the charge controller is a liquid crystal display Fig. 2, used for system control.
There are two buttons, the backlight and the output system selection button: Wind/Solar/Combined. It also has a charge selection switch to switch between battery charging mode and non-charging mode[21].

Fig. 3 The liquid crystal display of the charge controller is integrated with the front panel control console, which includes its connection terminal.

The system selection button displays the current and power generated by either one or both generators on the first line.
The second line indicates the amount of energy recovered by the battery in ampere-hours and the time it took. The third and fourth lines indicate the voltage for each connected battery and the type of current load. The system is autonomously powered by the battery/sun/wind.
There is 1 terminal for connecting the photovoltaic panel and 1 terminal for connecting the wind turbine. The panel also offers the possibility of connecting 2 batteries simultaneously[20].

3.2 Installation, commissioning, and operation procedure:

The mini wind turbine should be placed in an unobstructed location, with sufficient space behind the device to avoid airflow disruption (i.e., not placed too close to a wall). The same recommendations apply to the fan intake.
The wind turbine is connected to the charge controller terminals labeled WG (see Fig. 3). BROWN wires are connected to the (+) POSITIVE terminal, and BLUE wires are connected to the (-) NEGATIVE terminal.
The fan should be positioned in alignment with the wind turbine, initially at a zero-degree angle, and at a minimum distance of 500mm from the transparent protective cover.
To control the direction in which the fan points, it can be rotated, ensuring that the positions and angles are correct to maintain an airflow perpendicular to the blades. Test results can be obtained with the wind turbine directly facing the wind, or alternatively, with a slight angle relative to the wind to measure the effect of wind orientation on power production.
To control the wind speed, the fan and the wind turbine can be moved away from each other to reduce airspeed or brought closer to increase it.
Fig.4 illustrates the experimental setup for wind turbine operation. The advantage of a laboratory-based system is that the wind can be continuously controlled. This means that data can be collected at any time, rather than relying on weather forecasts[23].

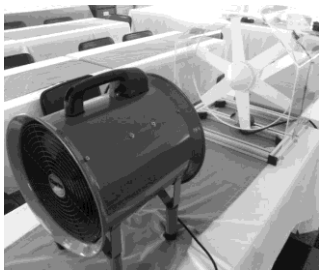

Fig. 4 Wind Turbine Functionality Test

All-important data is collected from the digital instrumentation present on the charge controller and the analog voltmeter, which is primarily used to observe the voltage increase when the wind turbine is not connected to the charge controller, as will be seen later[24].

3.3 Measurements

The results of measurements from various experiments are presented in this section. It should be noted that due to variations in local operating conditions (voltage and frequency of the mains power), weather conditions, and altitude, the test results obtained for each region and each device will vary significantly.

4 Scenario of the experiment

Table Tab.1 provides the results of the experiment conducted at the Renewable Energy Laboratory at NAAMA University Center in March 2021. For this experiment, in order to not depend on the nominal voltage of 12 volts imposed by the charge controller (which is exceeded, especially for high wind speeds), an ammeter was used to measure the current I in amperes. The voltage is directly read on the voltmeter of the wind turbine housing.
The electrical power generated by the wind turbine, and thus the product $P_{electrique}$ = I*Vt (watts), where Vt is the voltage displayed on the voltmeter of the wind turbine in volts.

Temp (°C)	V (mph)	N (tr/min)	Vt (Volt)	I (Amp)	Pelc (Watt)
20.6	6	320	5	0,01	0,05
	7	480	9,9	0,08	0 ,792
	9	540	9,9	0,2	1,98
	14	623	10	0,48	4 ,8
	29	700	11	0,75	8,25

Tab. 1: Results of the experiment.

4.1 Observations on the results of the experiment

Due to turbulence, the wind speed varies, especially at higher speeds, which leads to variations in voltage and current. The First measurement points correspond to moments when the current is most stable.
Wind speed is measured in mph (miles per hour) and has been rounded to the nearest integer, similar to the meteorological data we collect[27]. This rounding does not affect the measured power values.
As stated in the manual, the variation in wind speed in the laboratory is achieved by moving the fan closer or farther away. The lowest achievable wind speed (by moving the fan away) is 6 mph. This is not a problem since the wind turbine does not generate any power below this speed.
The maximum wind speed achieved by moving the fan closer is 29 mph. Higher speeds could be obtained using a second fan, but that would create excessive turbulence that would not be

representative of real-world conditions. An extrapolation (see Figure 3.7) will be used to estimate the corresponding power values for higher wind speeds encountered in the field (at lower frequencies).
The figure below depicts the electrical power generated by the wind turbine as a function of wind speed during the experiment. The resulting regression function has a logarithmic shape and exhibits a 99.7% correlation with the experimental data.
This function could be used in the Results and Discussion section for estimating the power corresponding to higher wind speeds encountered in the field (at lower frequencies).

4.2 Second Experiment Scenario: Utilization of the Charge Regulator

The use of the charge regulator fixes the voltage at either 12 or 24 volts Fig. 4. We observed that in the absence of batteries, this voltage is not as stable. It varied from 9 to approximately 21.9 volts, which is up to -3 volts from the nominal values.

The charge regulator has the advantage of displaying real-time power, voltage, and current generated by the wind turbine Fig. 5. When combined with the anemometer, we obtained the following results for the experiments conducted in July 2021

Experiment No. 1				
Temp (°C)	Wind speed (mph)	Current (Amp)	Voltage (Volt)	Power (Watt)
25.8	[7.7 8]	[0.07 0.09]	[13.4 13]	[0.94 1.2]
25.8	[9.9 11]	[0.12 0.15]	[21.8 21.5]	[2.66 3.2]
26	[13.6 15.3]	[0.4 0.54]	[10.2 09.1]	[4.1 4.89]
Experiment No. 2				
26.6	[13.3 14.8]	[0.26 0.37]	[13.2 12.7]	[3.8 4.67]
26.7	[14.6 15.6]	[0.32 0.41]	[13.9 12.7]	[4.5 5.2]
26.6	[13.3 14.8]	[0.26 0.37]	[13.2 12.7]	[3.8 4.67]

Tab. 2 Results of the second experiment

Fig. 5 Voltage set by the charge regulator at 12V or 24V

4.3 Comparison between the results of experiments and tests

Experiments 1 and 2 were conducted at different times of the year (spring, March, for Experiment 1, and summer, July, for Experiment 2), resulting in a temperature difference in the laboratory. This change in temperature affects the available wind power by modifying the air density according to the following formula [30]:

$$\rho = \frac{353,049}{Te} . e^{-0,034.\frac{Z}{Te}} \qquad \text{Equation 5}$$

Where Z is the site elevation in meters (m) and Te is the temperature in Kelvin. For the Naama University Center site located at an elevation of 1172 m, as indicated by google [27], the formula becomes:

$$\rho = \frac{353,049}{Te}.e^{\frac{-39,848}{Te}} \qquad \text{Equation 6}$$

Indeed, higher temperature leads to lower air density. However, this variation does not significantly affect the available wind power as the swept area by our mini wind turbine is relatively small (less than 0.2 m^2).
Note:

Despite the temperature variation between test 1 and test 2, no difference in power extraction is observed. Hence, these results can be combined in a single graph.
Figure 3.10 represents the electrical power generated by the mini wind turbine as a function of wind speeds during the second experiment. The resulting regression function has a logarithmic shape and shows 98.78% correlation with the experimental data.
Similar to the first experiment, this function could be used in the results and discussion section to estimate the powers corresponding to high wind speeds found in the profile but at low frequencies.

However, it should be noted that this extrapolation does not provide a power value for 6 mph, as in the first experiment. This is normal because hotter air, which is lighter, requires higher speeds to rotate the wind turbine.

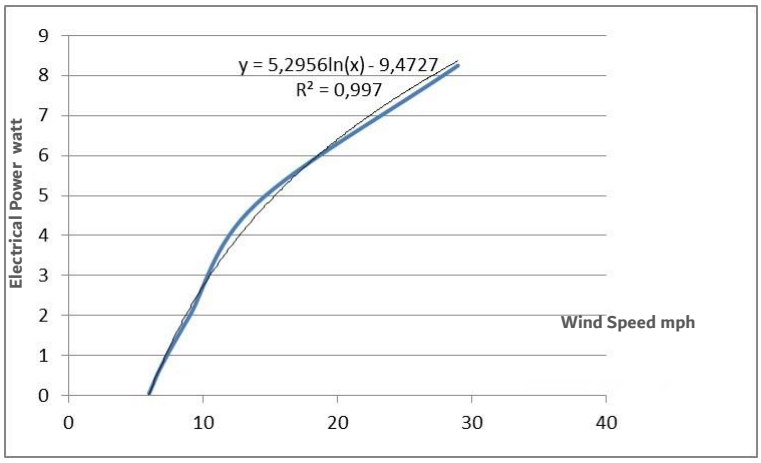

Fig. 6 Electrical Power as a Function of Wind Speed: Results of the First Experiment.

5 Results and Discussion

Figure Fig.6 presents the response curves of the wind turbine for experiments 1 and 2, at average temperatures of 20.6°C and 26.2°C, respectively.
These curves are obtained through trend analysis. Therefore, they are more accurate near the measurement points than further away (from 6 to 29 mph for experiment 1 and from 7.7 to 15.6 mph for experiment 2).
With correlation rates of over 99%, these curves show average relative errors around the measurement points of 18.07% and 4.51% respectively.
The difference in average relative error arises from the increase in the number of measurement points for experiment 2, the use of an interval rather than a representative rounded value, and

most importantly, the use of the charge regulator, which provides more accurate values. Nevertheless, both curves remain very close to each other and exhibit the same shape (same trend).

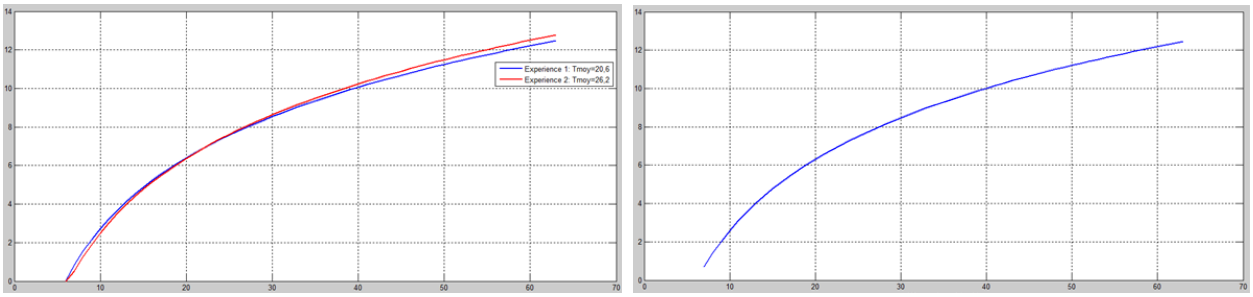

Fig. 7 Electric power response curves P_electric=f(V) of the small wind turbine.

It is also noticeable that the two curves intersect at V = 21.6 mph and have a maximum difference of 0.32 Watt at V = 7 mph.
Temperature has little influence on the wind turbine, primarily due to its small surface area (S = 0.196349541 m^2). Hence, the decision to plot the curve for all combined results, in accordance with the formula found in the measurement section (Fig. 7).

The startup wind speed of the wind turbine is theoretically obtained by solving the equation:

$$P\_electric = f(\text{Wind speed}) = 0 \qquad \text{Equation 5}$$

The results obtained for the three curves are: 5.9826 mph, 6.3936 mph, and 6.1582 mph, respectively. These results confirm those of the third experiment, which places the startup speed of our wind turbine in the range [5.55, 6.31] mph.
The small variations in this speed can be easily explained by the temperature variation. The hotter the air, the more speed (power) is needed to rotate the wind turbine: 5.98 mph at 20.6°C, [5.55, 6.31] mph at 24.7°C, and 6.39 mph at 26.2°C.
Note: The temperature in semi-desert regions such as the city of Naama, targeted by this study, ranges from -10°C in winter to over 50°C in the height of summer. For a better energy forecast and a more accurate estimation of the annual electrical power that could be produced by the wind turbine, the variation of the startup speed and the response curve with respect to temperature should be added to the model.
The figure below shows the annual statistical distribution of wind speeds in the study region (see the Statistical Data Analysis section).
The sum of wind hours with speeds of at least 7 mph (the speed at which our micro wind turbine begins to produce electricity) is 64.42% of the year, which is almost 236 days. In contrast, if we start counting from 11 mph, it accounts for only 40.46% of hours, equivalent to 148 days. Indeed, a region is considered ideal for wind application if the wind speed exceeds 4.75 m/s and remains stable throughout the seasons [29]. This significantly affects the wind potential of the study region.

Indeed, the small wind turbine used in this experiment has six blades. On this type of small turbines, it is better to use more blades to lower the startup speed, unlike large installations where using more than three blades is quite inefficient.
For the three response curves, the modes are respectively 12 mph, 13 mph, and 13 mph, with annual productions at these speeds averaging around 1.6 kWh.
The total energy produced over the year amounts to 21.7490 kWh, 20.8271 kWh, and 21.0939

kWh, equivalent to 59.4234 Wh, 56.9046 Wh, and 57.6335 Wh per day (considering all 366 days of the year, not just the equivalent hours of the 236 days with wind speeds of at least 7 mph). Statistically, this distribution tells us that the average energy produced at different wind speeds is m = 329.6 Wh, ranging from a minimum of 0 Wh to a maximum of 1567 Wh (achieved at the mode V=13 mph), with a standard deviation σ = 519.1 Wh.
We can observe that the mean is skewed to the left (relative to the min and max values), which is expected as we already knew that lower speeds are more frequent. This result is confirmed by a positive skewness coefficient: skew = 1.4009. A kurtosis coefficient of 3.3755 indicates that the distribution is somewhat stretched.
Finally, considering a maximum wind speed of 42 m/s for the class IV wind speeds to which our study region belongs, a rated speed of 5.81152 m/s (the mode 13 mph of the energy distribution), and a startup speed of 2.68224 m/s (solution of equation 3.9), formula 3.5 estimates the capacity factor at FC = 26.98% (>25%).

6 Conclusions

In addition to the previous information, it is important to note that the startup speed of the wind turbine, as determine d in the third experiment, falls within the range of [5.55, 6.31] mph. These results are consistent with the findings ob tained from the three curves, which measured speeds of 5.9826 mph, 6.3936 mph, and 6.1582 mph, respectively.

Furthermore, it should be considered that the startup speed of the wind turbine can vary due to temperature fluctuatio ns. As observed in the experiments, the startup speeds were 5.98 mph at 20.6°C, [5.55, 6.31] mph at 24.7°C, and 6.3 9 mph at 26.2°C. Given that the study region experiences a wide temperature range, ranging from −10°C in winter to over 50°C in summer, it is crucial to incorporate the variation of startup speed and response curve with respect to te mperature into the model. This will enhance the accuracy of energy forecasts and improve the estimation of annual el ectrical power production by the wind turbine.

Moreover, the annual statistical distribution of wind speeds in the study region is depicted in a figure, indicating that wind speeds of at least 7 mph, the threshold at which the micro wind turbine begins to generate electricity, occur for approximately 64.42% of the year (equivalent to around 236 days). However, if we consider a higher wind speed thre shold of 11 mph, it accounts for only 40.46% of the hours, corresponding to approximately 148 days. These statistics highlight the importance of wind speed stability and indicate the impact it has on the wind potential of the study regio n.

Additionally, it is worth noting that the small wind turbine used in the experiment features six blades. Unlike larger in stallations, which are generally inefficient with more than three blades, using more blades on small turbines helps low er the startup speed.

The analysis of the response curves reveals that the modes for the three curves are 12 mph, 13 mph, and 13 mph, wi th average annual productions of approximately 1.6 kWh at these speeds. Consequently, the total energy produced ov er the year amounts to 21.7490 kWh, 20.8271 kWh, and 21.0939 kWh, which is equivalent to 59.4234 Wh, 56.9046 Wh , and 57.6335 Wh per day, considering all 366 days of the year, rather than just the hours corresponding to the 236 d ays with wind speeds of at least 7 mph.

The statistical distribution further indicates that the average energy produced at different wind speeds is m = 329.6 W h, ranging from a minimum of 0 Wh to a maximum of 1567 Wh (achieved at the mode V=13 mph). The distribution exh ibits a positive skewness coefficient of skew = 1.4009, indicating a leftward skew due to the greater frequency of low er wind speeds. Moreover, the kurtosis coefficient of 3.3755 suggests that the distribution is somewhat stretched.

Finally, considering a maximum wind speed of 42 m/s for the class IV wind speeds applicable to the study region, a ra ted speed of 5.81152 m/s (corresponding to the mode 13 mph of the energy distribution), and a startup speed of 2.68 224 m/s (solving equation 3.9), formula 3.5 estimates the capacity factor at FC = 26.98%, which exceeds the 25% thre shold. This calculation demonstrates that the wind turbine in question achieves a favorable capacity factor, indicating its potential for efficient energy production.

7 References

[1] Jacobson, M. Z., & Archer, C. L. (2012). Saturation wind power potential and its implications for wind energy. Proceedings of the National Academy of Sciences, 109(39), 15679-15684.
[2] Abdullah, S., Jafri, M. Z., Mokhlis, H., Bakar, A. H. A., & Kadir, M. Z. A. A. (2017). Wind speed and wind power forecasting using local recurrent neural network. Renewable Energy, 105, 218-227.
[3] Jain, S., Kumar, D., & Kumar, A. (2018). Wind energy assessment and prediction using Weibull distribution: A case study for Rajasthan, India. Journal of Cleaner Production, 174, 836-845.
[4] Alsaad, M. A., Kavianpour, M., & Javid, A. H. (2019). Wind speed forecasting using hybrid artificial intelligence models: A review. Renewable and Sustainable Energy Reviews, 113, 109287.
[5] Akpinar, E. K., & Akpinar, S. (2005). An assessment on seasonal analysis of wind energy characteristics and wind turbine characteristics. Renewable Energy, 30(9), 1453-1471.
[6] Karabiber, A., & Ozerdem, B. (2021). Forecasting wind energy potential using deep learning algorithms. Energy Reports, 7, 1561-1568.
[7] Ghorbaniasl, G., Mohammadi, K., & Abedi, M. (2015). Wind speed forecasting using support vector regression and adaptive neuro-fuzzy inference systems. Renewable Energy, 83, 1042-1052.
[8] Bakshi, S., & Chandel, S. S. (2016). Prediction of wind energy potential using artificial neural network technique. International Journal of Sustainable Energy, 35(6), 536-551.
[9] Aydin, M., & Tanriverdi, M. (2014). Wind speed and power forecasting using hybrid models. Renewable Energy, 68, 193-204.
[10] Adaramola, M. S., Oyewola, O. M., & Paul, S. S. (2012). Assessment of wind characteristics and wind energy potential of Ogun State, Nigeria. Applied Energy, 97, 355-362.
[11] Akdag, S. A., Ecevit, A., & Erhan, E. (2019). Forecasting of wind speed using statistical and artificial intelligence methods. Renewable Energy, 135, 1359-1372.
[12] Sailor, D. J. (2008). A review of methods for estimating anthropogenic heat and moisture emissions in the urban environment. International Journal of Climatology, 28(7), 973-989.
[13] Akselrod, M., & Pechkis, H. (2018). A comprehensive review of wind turbine power curves. Renewable and Sustainable Energy Reviews, 81, 2162-2172.
[14] Ruiz-Arias, J. A., Gueymard, C. A., Pozo-Vázquez, D., Tovar-Pescador, J., & Santos-Alamillos, F. J. (2009). Generation of typical meteorological years for 26 sites in Spain using the ERA-40 reanalysis. Solar Energy, 83(10), 1761-1772.
[15] Bossanyi, E. (2003). The design of closed-loop controllers for wind turbines. Control Engineering Practice, 11(3), 307-316.
[16] Glavitsch, H. (2005). Assessment of wind power uncertainty caused by short-term prediction errors. Wind Energy, 8(4), 403-417.
[17] Devabhaktuni, V. K., Alam, M., Depuru, S. S., Green, R. C., Nims, D., & Near, C. (2013). Solar energy: Trends and enabling technologies. Renewable and Sustainable Energy Reviews, 19, 555-564.
[18] Infield, D. G., & Lave, M. (2008). Energy generation from wind: Comparative analysis of environmental performance. Journal of Power Sources, 185(2), 665-672.
[19] Morthorst, P. E. (2000). Green certificates in the electricity market. Energy Policy, 28(14), 1047-1059.
[20] Carta, J. A., Ramírez, P., & Velázquez, S. (2009). Analytical approximation for wind speed distribution in the atmospheric boundary layer. Solar Energy, 83(9), 1645-1656.
[21] Holttinen, H., Sillanpää, S., Weir, D., Kiviluoma, J., & Milligan, M. (2013). Operating reserves and wind power integration. Wind Energy, 16(2), 283-297.
[22] Carlini, E. M., & Nelson, V. A. (2010). Decomposing the variability of wind and solar for stochastic unit commitment. IEEE Transactions on Power Systems, 25(2), 1179-1190.
[23] Meng, Y., Qu, X., Huang, X., & Zhang, Q. (2014). Wind energy integration and associated risk assessment in deregulated power markets. International Journal of Electrical Power & Energy Systems, 55, 154-161.
[24] Canizares, C., & Bhattacharya, K. (2005). Optimal unit commitment with wind and storage. IEEE Transactions on Power Systems, 20(1), 114-124.
[25] Sathe, A., Mandal, P., & Prasad, D. (2012). Technological advances in wind turbine design. Renewable Energy, 37(1), 1-12.
[26] Holttinen, H., & Laaksonen, V. (2006). Impact of wind power on power system dynamics and operation. Wind Energy, 9(2), 109-129.
[27] De Groot, A. M., & Saric, S. (2004). Power smoothing of wind farms by adding energy storage. Wind Energy, 7(1), 47-55.
[28] Olauson, J. (2007). Wind turbines: noise assessment, prediction and control. Environmental Impact Assessment Review, 27(2-3), 190-207.
[29] Mendoza, V. E., Cruz, J. L., & Portilla, J. (2012). A review on the development and properties of continuous rotor wind turbines. Renewable and Sustainable Energy Reviews, 16(5), 2824-2837.
[30] Chai, T., & Draxl, C. (2010). Validation of wind speed and power measurements for NREL's state-of-the-art wind turbine data. Journal of Solar Energy Engineering, 132(1), 011009.